Antimony isotopic composition in river waters affected by ancient mining activity

Eléonore Resongles, Remi Freydier, Corinne Casiot, Jerome Viers, Jérôme Chmeleff, Françoise Elbaz-Poulichet

Antimony isotopic composition in river waters affected by ancient mining activity

Eléonore Resongles[a*], Rémi Freydier[a], Corinne Casiot[a], Jérôme Viers[b], Jérôme Chmeleff[b] and Françoise Elbaz-Poulichet[a]

[a]HydroSciences UMR CNRS 5569 – IRD 050 – Université de Montpellier, CC0057, 163 rue Auguste Broussonet, 34090 Montpellier - France

[b]Géosciences Environnement Toulouse UMR CNRS 5563 – Université Toulouse III – IRD 234, 14 Avenue Edouard Belin, 31400 Toulouse, France

*Corresponding author:

Tel.: +33467143605
E-mail address: eleonore.resongles@univ-montp2.fr

ABSTRACT

In this study, antimony (Sb) isotopic composition was determined in natural water samples collected along two hydrosystems impacted by historical mining activities: the upper Orb River and the Gardon River watershed (SE, France). Antimony isotope ratio was measured by HG-MC-ICP-MS (Hydride Generation Multi-Collector Inductively Coupled Plasma Mass Spectrometer) after a preconcentration and purification step using a new thiol-cellulose powder (TCP) procedure. The external reproducibility obtained for $\delta^{123}Sb$ measurements of our in-house Sb isotopic standard solution and a certified reference freshwater was 0.06‰ (2σ).

Significant isotopic variations were evident in surface waters from the upper Orb River ($-0.06‰ \leq \delta^{123}Sb \leq +0.11‰$) and from the Gardon River watershed ($+0.27‰ \leq \delta^{123}Sb \leq +0.83‰$). In particular, streams that drained different former mining sites exploited for Sb or Pb-Zn exhibited contrasted Sb isotopic signature. Additional work will be performed to determine Sb isotopic signature of rocks, mine wastes and sediments in order to fully understand these Sb isotopic variations. Furthermore, experimental work is needed to characterize Sb isotope fractionation resulting from the different biogeochemical processes which may impact Sb isotopes during rock weathering and Sb transport in surface waters. Nevertheless, Sb which was present in Sb(V) form in oxic surface waters appeared to have a conservative behavior along the Gardon River, allowing for the use of Sb isotopes as a source tracer. This study suggests that Sb isotopic composition could be a useful tool to track pollution sources and/or biogeochemical processes in hydrologic systems.

Keywords

Antimony isotopes; thiol-cellulose powder TCP; hydride generation; MC-ICP-MS; river water; mining pollution

1. Introduction

Human activities have induced important changes in metal and metalloid cycles. Among these elements, antimony (Sb) is of great concern: its anthropogenic fluxes largely exceed Earth's surface natural fluxes, mining being the major factor (> 90%) of anthropogenic influence (Klee and Graedel 2004; Sen and Peucker-Ehrenbrink 2012). As a consequence of Sb mining, smelting, industrial processing and waste disposal, severe enrichments with Sb have been reported in rivers, estuaries, atmospheric aerosols, soils, peat bogs, alpine and polar snow and ice (Byrd 1990; Shotyk et al. 1996, 2004, 2005; Filella et al. 2002a; Cloy et al. 2005; Krachler et al. 2005; He et al. 2012; Hiller et al. 2012; Hong et al. 2012). Freshwater systems are particularly affected by Sb contamination as reflected by the classification of Sb for nearly four decades among pollutants of priority interest in waters by the Environmental Protection Agency of the United States and the European Union (USEPA 1984; CEC 1976). Antimony enters in freshwater systems through rock weathering and soil leaching. Dissolved Sb concentration ranges generally from few $ng.L^{-1}$ to less than 1 $\mu g.L^{-1}$ in uncontaminated freshwater systems (Filella et al. 2002a). However, it can reach hundreds $\mu g.L^{-1}$ in polluted rivers, especially close to current or former mining sites and smelters (Filella et al. 2002a, 2009; Casiot et al. 2007; Liu et al. 2010; Wang et al. 2011; Asaoka et al. 2012; He et al. 2012; Hiller et al. 2012; Resongles et al. 2013). In this context, Sb sources and behavior need to be fully understood to predict its potential mobility, bioavailability and toxicity in aquatic environments and to initiate relevant remediation plans in mining-affected hydrosystems. In this sense, the geochemistry of Sb stable isotopes could be a powerful tool to elucidate sources and/or biogeochemical processes in hydrosystems as already demonstrated for other metal contaminants such as Cu, Hg and Zn (e.g. Weiss et al. 2008; Borrok et al. 2009; Foucher et al. 2009; Kimball et al. 2009).

Antimony has two stable isotopes, ^{121}Sb and ^{123}Sb with average abundances of 57.213% and 42.787% (Chang et al. 1993). To date, little investigation have been done on the Sb isotope system (Rouxel et al. 2003; Asaoka et al. 2011; Tanimizu et al. 2011; Lobo et al. 2012, 2013, 2014). Although the absolute values of $\delta^{123}Sb$ obtained in these different studies cannot be compared to each other because the authors used different in-house Sb isotopic standard, significant variations of Sb isotopic composition has been reported in various geological, environmental and anthropogenic samples. The extent of Sb isotopic composition variations depends on the sample type: the largest range of $\delta^{123}Sb$ values (up to 1.8‰) was

found in hydrothermal sulfides while a more limited range was determined in the continental and oceanic crust reservoir (variation about 0.3‰) and the North Atlantic seawater; the latter had a homogeneous δ^{123}Sb value of 0.37 ± 0.04‰ (Rouxel et al. 2003). For stibnite, the main exploited Sb ore, a variation spanning 1.0‰ has been observed (Lobo et al. 2012), allowing for the use of Sb isotope ratio as a proxy for provenance determination of ancient and Roman glass in which Sb is added either as a decolorizer or as an opacifier (Lobo et al. 2013, 2014). Furthermore, Sb isotope fractionation has been observed during the abiotic reduction of Sb(V) into Sb(III) (Rouxel et al. 2003), predicting an important role of redox transformations regarding Sb isotope system. However, very little information is available on Sb isotopic composition in river waters (Asaoka et al. 2011; Tanimizu et al. 2011).

The objective of this study was to evaluate the possible use of Sb isotopes to constrain sources and/or geochemical processes in hydrosystems impacted by former mining sites. For this, we analyzed Sb isotopic composition of river waters from the upper Orb and Gardon River watersheds, in Southern France. Analysis was carried out using MC-ICP-MS coupled with hydride generation, after sample purification using thiol-cellulose powder (TCP), according to a procedure adapted from Rouxel et al. (2003) and Asaoka et al. (2011). Finally, we discussed potential sources and/or geochemical processes which could have affected Sb in the studied hydrosystems.

2. Study sites and sample locations

Natural water samples were collected along two rivers located in the south-eastern flank of the French Massif Central Mountains. The area has been mined for metals (Pb, Zn, Ag) and Sb for centuries, until the mid-20th century. As a consequence, tens of abandoned extraction and ore processing sites are still contaminating surface waters with metals and metalloids (e.g. Casiot et al. 2007, 2009; Resongles et al. 2014). Among these elements, Sb is of great concern in the area; Sb concentration reaches 32 µg.L^{-1} in the small river downstream from the Sb mine of Bournac (Casiot et al. 2007), 410 µg.L^{-1} downstream from the Pb-Zn mine of Carnoulès (Resongles et al. 2013) and 11 µg.L^{-1} along the upper Gardon of Alès River where both Sb and Pb-Zn have been mined (Resongles et al. under review). In this last area, there are aquifers supplying small villages that occasionally exceed drinking water standards (5 µg.L^{-1}) (ARS website). Surface water samples were collected at 3 stations along the upper Orb River (Figure 1a) and at 10 stations throughout the Gardon River watershed (Figure 1b).

The upper Orb River drains the former Sb mine of Bournac where ~600 t of Sb were extracted in the form of stibnite (Sb_2S_3) between 1908 and 1920 (Munoz and Shepherd 1987). The Bournac Creek (O1) drains the mineralized area and flows next to a tailing heap where dissolved Sb concentration as high as 32 µg.L^{-1} has been measured (Casiot et al. 2007). The Avene Lake (O2) located on the course of the Orb River (O3) receives waters from the Bournac Creek (Figure 1a).

The Gardon River watershed drains numerous former mining sites including an important Sb mine (Felgerette) as well as coal, pyrite and Pb/Zn mines (Figure 1b). At the Felgerette mine, 2570 t of Sb were extracted as stibnite between 1906 and 1948 leaving 38 000 t of mining residues (BRGM, SIG Mines website). Stations T1 to T4 correspond to tributaries impacted by old mining activities, some of them also drain urban (T2) or industrial (T3) areas. The Ravin des Bernes Creek (T1), the Grabieux River (T2) and the Avène River (T3) join the Gardon of Alès River (G1 to G5) while the Amous River (T3) joins the Gardon of Anduze River (T5). The station G6 is situated downstream from the confluence between the Gardon of Alès and the Gardon of Anduze Rivers (Figure 1b). Additionally, a sample of tap water was collected at the Collet de Deze village on the Gardon River watershed (DW, Figure 1b). This drinking water originates from the alluvial aquifer of the Dourdon and the Gardon of Alès Rivers and exhibits relatively high dissolved Sb concentrations (up to 8.0 µg.L^{-1} between 2010 and 2012, with an average of 2.8 µg.L^{-1}, n=13, ARS website).

3. Materials and methods

3.1. Sample collection and field measurements

Water samples for Sb and trace element concentration determination and Sb isotope analysis were collected in 2 L HDPE bottles and filtered upon return to the laboratory through 0.22 µm membranes (Millipore) fitted on polycarbonate filter holders (Sartorius). Filtered samples were stored in other 2 L HDPE bottles, acidified to 0.01 M with Suprapur® 14.5 M HNO3 (Merck) and kept at 4 °C. Samples for Sb speciation were filtered in the field using a syringe and a disposable 0.22 µm cellulose acetate syringe filter and collected in polypropylene tubes, they were brought in a cool box and they were analyzed upon return to the laboratory. The samples for the determination of major anions (F-, Br-, Cl^-, NO_3^-, SO_4^{2-}, CO_3^{2-}, HCO_3^-) and cations (Ca^{2+}, Mg^{2+}, Na^+, and K^+) were sampled and preserved according to the routine procedures described in Casiot et al. (2009). The pH, conductivity and dissolved oxygen concentration (DO) were measured using an HQ40d Portable Multi-Parameter Meter (HACH Company) equipped with a refillable pH electrode (pHC301), conductivity electrode (CDC401) and a Luminescent DO probe (LDO101).

3.2. Materials and reagents

Sample processing was carried out in a class 10,000 clean lab equipped with a class 100 laminar-flow clean bench. MilliQ water (resistivity >18.2 MΩ, Q-POP Element system, Millipore) was used for all experiments and reagent preparations. All materials (e.g. sample bottles, test tubes, centrifuge tubes, columns, pipette tips,…) were washed before use in a bath of 20% HCl of analytical grade for 48 h and rinsed three times with Milli-Q water.

Antimony preconcentration and purification procedure was performed using 10 mL polypropylene columns (active length 4 cm, diameter 0.8 cm, Bio-Rad) and a vacuum manifold (57044 Visiprep-DL 12, Supelco) which allows processing 12 samples simultaneously and controlling the flow rate.

For the preparation of thiol-cellulose powder, 20 µm microcrystalline cellulose powder was used (Sigma-Aldrich) and was modified using thioglycolic acid (98%, Sigma-Aldrich), analytical grade acetic anhydride (98%, Chem-Lab), analytical grade acetic acid (99-100%, Chem-Lab) and analytical grade sulfuric acid (95-98%, Merck). Suprapur® 30% HCl (Merck)

was used for eluent and experimental solution preparation and for water sample acidification. A solution containing a mixture of analytical grade ascorbic acid (Sigma-Aldrich) and Suprapur® potassium iodide (Merck) was prepared daily; it was used for the reduction of Sb(V) in synthetic solutions and in natural water samples. Hydride generation reagent was daily prepared by mixing 1% (w/v) sodium borohydride and 0.05% (w/v) sodium hydroxide (both 99.99% trace metal basis, Sigma-Aldrich). Single element standard solutions (As, Ge, Sb, Se, Sn, Te) at 1000 $\mu g.mL^{-1}$ used for procedure validation and in-house Sb isotopic standard were both purchased from SCP Science. For the Sb isotopic standard, the exact reference is: SCP Science, PlasmaCAL ICP/ICPMS Standard - Antimony 1000 $\mu g.ml^{-1}$, lot number SC0108283.

3.3. Sample preparation for Sb isotope ratio analysis

3.3.a. Preparation of thiol-cellulose powder

Thiol-cellulose powder (TCP) was prepared using the procedure described by Rouxel et al. (2003) for thiol-cotton fiber (TCF). Thioglycolic acid (62.6 mL), acetic anhydride (34.7 mL), acetic acid (16.5 mL) and sulfuric acid (0.137 mL) were mixed successively in a 500 mL PTFE wide mouth bottle and the mixture was homogenized and allowed to cool to room temperature. Then, 10 g of cellulose powder was added and after gently stirring, the bottle was closed and left for 4 days in a water bath at 40 °C with daily stirring. Finally, the acid mixture was removed and the TCP was washed 10-times with Milli-Q water by centrifuging (2000 rpm for 5 min) and removing the supernatant between each rinse. The TCP was transferred in a clean box and dried at room temperature under a laminar-flow clean bench for 2 days. TCP was stored at room temperature (~20 °C) in a sealed opaque box.

3.3.b. Sb preconcentration and purification procedure

Synthetic solutions and natural water samples were brought to 0.5 M HCl, then Sb(V) was reduced into Sb(III) by adding a suitable amount of 10% (w/v) KI-ascorbic acid solution to obtain a final concentration in sample of 0.5% (w/v). This reduction step is required to ensure a total adsorption of Sb on TCP due to the low adsorption rate of Sb(V) on thiol groups (Yu et al. 1983). The reduction time was fixed at 3h, providing a 98% Sb(V) reduction (Asaoka et al. 2011). .

Antimony preconcentration and purification procedure (hereafter referred to as TCP procedure) was optimized for natural water samples using TCP following the works of Rouxel et al. (2003) and Asaoka et al. (2011); this optimized procedure is summarized in Table 1. Columns were set up on a vacuum manifold and filled with 0.7 mL of TCP (wet volume). The flow rate was fixed at 1.0 $mL.min^{-1}$ during the whole procedure and special care was taken to ensure that TCP never dried out. Firstly, TCP was washed with 25 mL of Milli-Q water and conditioned with 25 mL of 0.5 M HCl. Then, sample was loaded on TCP. It was demonstrated here that the final procedure yield averaged 99 ± 2% whatever the processed river water volume within the range 10 – 500 mL (Table 1, Supporting Information). Loading of high sample volumes may be necessary since a minimum of 20 ng Sb is required for isotopic analysis. Antimony and other elements which exhibit high adsorption capability in 0.5 M HCl medium (e.g. Sn, As) are retained on TCP while major ions and metals are expected to pass through the column and to be retrieved in fraction A (Table 1), (Yu et al. 2001, 2002). Then, TCP was washed successively with 5 mL of 0.5 M HCl and 6 mL of 2.5 M HCl (fractions B and C, Table 1) to remove residual matrix elements and Sn, respectively (Asaoka et al. 2011). After the second wash, remnant liquid was purged out from the TCP column. The efficiency of the TCP procedure in removing interfering elements was checked on the certified water NIST SRM 1643e and an experimental solution spiked with As, Ge, Sb, Se, Sn and Te at 50 $\mu g.L^{-1}$ each (Table 2, Supporting Information). Extraction of Sb from TCP was carried out after TCP transfer into a 15 mL centrifugation tube (blowing with a clean gas (N_2) at the bottom of the column) using 3 mL of 6 M HCl followed by ultrasound treatment (15 min), then centrifugation (4000 rpm, 20 min) and supernatant collection. Three successive extraction steps were sufficient to achieve a quantitative recovery of Sb (96 ± 2%, n=3) (Figure 1, Supporting Information). Supernatants recovered at each step were combined in the same 15 mL polypropylene centrifugation tube. Finally, sample was centrifuged at 4500 rpm for 30 min to remove possible cellulose particles and the final extract (~9 mL) was retrieved in a polypropylene test tube and stored at 4 °C until analysis (fraction D, Table 1).

Procedural blanks consisting of MilliQ water treated as a water sample with the entire TCP procedure were performed to ensure that no Sb contamination occurred during the TCP procedure. Results showed that the amount of Sb in blank samples was lower than 0.15 ng (n=4). Considering that a minimal amount of 20 ng of Sb has to be preconcentrated on TCP column to allow subsequent isotopic analysis, procedural blank contribution represented less than 1% of total Sb.

Using this TCP procedure, Sb was quantitatively recovered (procedure yield = 96 ± 3%) from all river water samples analyzed during the course of this study. Moreover, more than 95% of every single potentially interfering element (Cd, Co, Ge, Pb, Se, As, Cu, Fe, Ni, Zn) was removed in purified simples (fraction D, Table 2, Supporting Information). Such purification was essential because metals (e.g. Cd, Co, Cu, Fe, Ni, Pb, Zn) and hydride-forming elements (e.g. As, Ge, Se, Sn, Te) can inhibit the formation of stibine (SbH_3) and/or lead to matrix effect during analysis (Yu et al. 1983; Kumar and Riyazuddin 2010; Henden et al. 2011).

3.4. Analysis

3.4.a. Determination of major and trace element concentrations and Sb speciation

Major cations, anions (F^-, Br^-, Cl^-, NO_3^-, SO_4^{2-}, Ca^{2+}, Mg^{2+}, Na^+, and K^+) and carbonate species (CO_3^{2-}, HCO_3^-) were analyzed as described in Casiot et al. (2009).

Trace elements and interfering elements were determined using ICP-MS (X Series II, Thermo Scientific) equipped with a collision cell technology chamber (CCT) ("Plateforme AETE" - HydroSciences/OSU OREME, Montpellier - France). Natural water samples were analyzed in 2.5% HNO_3 medium without dilution except for samples collected close to mining sites. Samples purified on TCP (fractions A, B, C and D, Table 1) were analyzed in 1.8% HCl medium after an adequate dilution. Quantitative analyzes were performed using external calibration with In as an internal standard to correct for instrumental drift and possible matrix effects. Certified reference waters (artificial freshwater NIST SRM 1643e and natural river water CNRC SLRS-5) were prepared in the same medium as samples and used to check analytical accuracy and precision. Measured concentrations were within 10% of the certified values and analytical error (relative standard deviation) was better than 5% for concentrations ten times higher than the detection limits.

Determination of dissolved Sb(III) and Sb(V) concentrations was carried out by High Performance Liquid Chromatography coupled to Inductively Coupled Plasma Mass Spectrometry (HPLC-ICP-MS) as described in Resongles et al. (2013).

3.4.b. Determination of Sb recovery from preconcentration and purification procedure

During the TCP procedure development, Sb recovery was quantified in the fractions collected at each step of the procedure (fraction A, B and C) and in the final extract (fraction D) in order to check efficiency and reproducibility of the procedure (Table 1 and SI, Table 2). In addition, procedure yield was systematically controlled in preconcentrated and purified samples before Sb isotopic analysis. For this purpose, continuous flow hydride generation (HGX-200 system, CETAC Technologies) was coupled with ICP-MS (XSeries II, Thermo Scientific) because it allows the determination of low Sb concentrations in 3 M HCl medium due to the enhancement of signal sensitivity. Aliquots of fraction A, B, C and D were brought to 3 M HCl and a 10% (w/v) KI-ascorbic acid solution was added to obtain a final concentration of 0.5% (w/v), at least 3h before analysis to reduce Sb(V) into Sb(III). This reduction step is required before analysis because hydride generation (HG) is selective for Sb(III) species (Kumar and Riyazuddin 2010). The reagent used for hydride generation was a solution of 1% (w/v) $NaBH_4$ stabilized in 0.05% (w/v) NaOH and filtered before use through 0.45 µm PVDF membrane fitted on a clean polycarbonate filter holders (Sartorius).

Operating conditions of HG system are detailed in Table 2. A micro peristaltic pump (MP^2, Elemental Scientific) was used for delivering the sample and the reducing agent into the HG system. A mixing coil enhances hydride formation and an Ar inlet allowed driving hydrides in a gas-liquid separator. A second peristaltic pump (Minipuls, Gilson) was used to drain the liquid waste out of the HG system. After the gas-liquid separator, a 1 µm PTFE membrane prevented the entry of aerosols into the ICP-MS torch and a second Ar inlet transported hydrides to ICP-MS.

ICP-MS settings are shown in Table 2. External calibration was performed. Certified reference freshwaters (NIST SRM 1643e from the National Institute of Standards and Technology and CNRC SLRS-5 from the Canadian National Research Council) were regularly analyzed to check analytical accuracy. Measured Sb concentration was within 5% of the certified values and analytical error (relative standard deviation) was better than 5% for concentrations ten times higher than the detection limit (DL = 0.01 $\mu g.L^{-1}$).

3.4.c. Antimony isotope ratio measurement

For Sb isotopic analysis, final extracts of the TCP procedure (fraction D) were brought to 3 M HCl with Milli-Q water and an appropriate dilution was performed to obtain a final Sb concentration of 1 µg.L^{-1}. A 10% (w/v) KI-ascorbic acid solution was added to bring the sample at a concentration of 0.5% (w/v) at least 3h before HG-MC-ICP-MS analysis to allow for Sb reduction.

Sb isotopic analyzes were performed using a multi-collector inductively coupled plasma mass spectrometer (MC-ICP-MS, Neptune, Thermo Scientific) at the Observatoire Midi-Pyrénées ICP-MS facility (Toulouse, France). The hydride generation system described above (section 3.4.b) was used as sample introduction system and coupled to the MC-ICP-MS as previously mentioned for Se (Rouxel et al. 2002; Elwaer and Hintelmann 2008) and Sb (Rouxel et al. 2003). Operating conditions for the HG system are detailed in Table 2; gas flow rates of the two Ar inlets in HG system were adjusted daily to improve sensitivity and signal stability. HG-MC-ICP-MS settings are presented in Table 2.

Sb isotopes (^{121}Sb and ^{123}Sb), two Sn isotopes (^{120}Sn and ^{122}Sn) and one Te isotope (^{126}Te) were monitored simultaneously (Table 2). Antimony signal intensity was 700-800 mV for the ^{121}Sb isotope and 500-600 mV for the ^{123}Sb isotope (Sb = 1µg.L^{-1}). ^{126}Te signal was measured to correct the potential isobaric interference of ^{123}Te on ^{123}Sb. Although Sn was quantitatively removed during TCP procedure, a signal of ~50 mV on ^{120}Sn isotope was detected for both blanks and samples. This Sn contamination probably originates from the reducing agent used for HG as reported by Rouxel et al. (2003). However, it did not appear to interfere with Sb isotopic analysis (Rouxel et al. 2003). A wash time of 2 min with 3 M HCl was sufficient to lower the signal value to background level between each analysis. Analytical blanks (0.5 M HCl, 0.5%w/v KI-ascorbic acid) were regularly analyzed (every 7 samples) in order to check the analytical background. Blank signal intensity represented less than 1.5% of the Sb signal measured in samples. This analytical background was subtracted from the ^{121}Sb and ^{123}Sb signal measurements for samples and standards. The internal error on ^{123}Sb/^{121}Sb ratio measurement was about 0.015% (relative standard deviation).

Each sample was analyzed three times and was bracketed with an in-house Sb standard solution prepared at the same concentration as samples (1 µg.L^{-1}). The instrumental mass bias was corrected using the standard-sample bracketing method. Antimony isotopic results are reported in δ^{123}Sb notation as recommended by IUPAC (Coplen 2011). δ^{123}Sb is defined as

the deviation between $^{123}Sb/^{121}Sb$ ratio in sample and the average of $^{123}Sb/^{121}Sb$ ratios of the bracketing standards, in per mil unit (Equation 1).

$$\delta^{123}Sb = \left(\frac{\left(^{123}Sb/^{121}Sb\right)_{sample}}{\left(^{123}Sb/^{121}Sb\right)_{standard\ average}} - 1 \right) \times 1000 \qquad \text{Eq. 1}$$

In order to check that the TCP procedure did not induce isotope fractionation and to assess analytical accuracy, Sb isotopic analyzes were performed on our in-house isotopic Sb standard solution treated with TCP procedure. Antimony recovery in the final extract was 94 ± 1% (n=3, 1σ) and $\delta^{123}Sb$ was 0.00 ± 0.03‰ (n=3 procedural replicates, 1σ). The certified reference water NIST SRM 1643e purified on TCP was also regularly analyzed, it was found at $\delta^{123}Sb$ = 0.16 ± 0.03‰ (n=5 procedural replicates, 1σ). Therefore, the external reproducibility obtained for NIST SRM 1643e water was used for all the isotopic results presented in this study: 2σ = 0.06‰ (SI, Table 3).

4. Results

4.1. Water hydrochemistry

Samples from the upper Gardon of Alès subwatershed (T1, G1, G2, DW) and from the Bournac Creek (O1) exhibited neutral pH (7.1 ± 0.2) and low conductivity (97 ± 23 $\mu S.cm^{-1}$) whereas other samples located at downstream sites along the Gardon and Orb watersheds had a higher pH (8.0 ± 0.3) and their conductivity was higher than 300 $\mu S.cm^{-1}$ (Table 3). These parameters together with major ion concentrations reflected the contrasted lithology from upstream to downstream parts of both watersheds, varying from schists (weakly mineralized waters at T1, G1, G2, DW, O1) to carbonate formations (higher concentrations of HCO_3, SO_4, Ca, Mg, Sr at downstream stations G3 to G6 and O2 to O3).

Most samples exhibited dissolved Sb concentration higher than 1 $\mu g.L^{-1}$ (Table 3), which denoted significant enrichment compared to typical concentrations less than 1 $\mu g.L^{-1}$ in uncontaminated waters (Filella et al. 2002a). The highest Sb values were recorded in the creeks that drained old Sb mines located on the uppermost course of the Gardon of Alès River (87.4 µg $Sb.L^{-1}$ at T1) and the Orb River (53.8 µg $Sb.L^{-1}$ at O1). Dissolved Sb concentrations were lower (0.5 – 1.9 µg $Sb.L^{-1}$) in the creeks that drained old Pb/Zn mines on the Gardon River watershed (T2, T3 and T4). In the upper Gardon of Alès River, dissolved Sb concentration was low (0.4 µg $Sb.L^{-1}$ at G1) and increased downstream from the Sb mineralized zone and the related Sb mine inputs (7.7 µg $Sb.L^{-1}$ at G2). Then, along the main course of the Gardon River, dissolved Sb concentration decreased from upstream to downstream stations (from 7.7 µg $Sb.L^{-1}$ at G2 to 1.2 µg $Sb.L^{-1}$ at G6). Downstream from the Bournac Sb mine, in the Avene Lake (O2) and in the main stream of the Orb River (O3), dissolved Sb concentration was close to 1 $\mu g.L^{-1}$. Antimony(V) was the only species detected in all samples, Sb(III) was lower than the detection limit (0.03 $\mu g.L^{-1}$), in agreement with thermodynamic equilibrium that predicted the predominance of Sb(V) in natural oxic waters (Filella et al. 2002b).

Interestingly, arsenic was encountered at high concentrations in tributaries impacted by Sb mines (17 µg $As.L^{-1}$ at T1; 90.4 µg $As.L^{-1}$ at O1) and Pb/Zn mines (2.6 µg $As.L^{-1}$ at T2; 9 µg $As.L^{-1}$ at T3; 10 µg $As.L^{-1}$ at T4), reflecting the strong association of these metalloids in sulfide minerals (Filella et al. 2002a). The dissolved concentrations of other trace elements in the mine-affected streams were in the same order of magnitude that world river average

values (Gaillardet et al. 2003), except Pb and Zn in the Bournac Creek (O1) downstream from the Bournac Sb mine, also Co, Mn, Ni and Zn in the Amous River (T4), that drains the Pb/Zn mine of Carnoulès (Casiot et al. 2009), and Mo, Ni, Rb, Ti, Tl, V and Zn in the Avène River (T3), that drains both Pb/Zn mines and an industrial center (Figure 1). This latter river also exhibited higher conductivity and major ion concentrations (Cl, NO_3, SO_4, Ca, K, Na) than other rivers. The Gardon of Alès River also presented elevated concentration of Zn and Mo downstream from the Alès town (G4 and G5) and the Avène River confluence (G5), respectively. The drinking water sample DW exhibited high Cu concentration, in relation with the use of copper line pipes for drinking water supply.

4.2. Antimony isotopic composition

4.2.a. Mine-affected streams

Antimony isotopic composition ($\delta^{123}Sb$) of the mine-affected streams ranged from -0.06 to +0.83‰ (Figure 2). It is noteworthy that the most Sb-rich creeks T1 and O1 that both drain former Sb mines (Felgerette and Bournac mine respectively, Figure 1) in the Gardon and Orb watersheds revealed the highest and lowest $\delta^{123}Sb$ values measured in this study (0.83‰ at T1, -0.06‰ at O1). Conversely, streams T3 and T4, that both drain former Pb/Zn mines on the Gardon of Alès and the Gardon of Anduze subwatersheds, exhibited a similar Sb isotopic signature: 0.33‰ (T3) and 0.27‰ (T4). However, Sb isotopic composition differed for stream T2 ($\delta^{123}Sb = 0.60 \pm 0.06$‰) that also drains Pb/Zn mines in the Gardon of Alès subwatershed. This denoted either variation in the isotopic signature of Sb in the ore material within a relatively small geographic scale, or fractionation of Sb isotopes during transfer of Sb from the original ore into water.

4.2.b. Orb and Gardon Rivers

Antimony isotopic composition measured throughout the Gardon River watershed (0.55 ± 0.21‰, n=12) differed significantly from the values obtained along the upper Orb River (0.03 ± 0.08‰, n=3). Moreover, Sb isotopic composition varied significantly within a single watershed: from 0.23 to 0.83‰ in the Gardon River watershed and from -0.06 to 0.11‰ in the upper Orb River watershed. This demonstrated that natural Sb isotopic variations are significant in river systems.

Antimony isotopic composition of the main stream of the Orb River differed from that of the Sb mine-affected stream (Figure 2a), with an increase of δ^{123}Sb signature from -0.06‰ in the Bournac creek (O1) to 0.03‰ in the Avene Lake located on the course of the Orb River (O2); then it further increased up to 0.11‰ in the Orb River downstream from the reservoir (O3). This suggests that the Bournac Creek was not the predominant source of Sb in the Orb River or that Sb isotope fractionation occurred during Sb transfer.

Along the Gardon River (Figure 2b), the Sb signature increased from 0.23‰ in the uncontaminated upper Gardon of Alès River (G1) to 0.74‰ (G2) downstream from the Sb mineralized zone and the Sb mine input (T1); it was allied to a 19-fold increase of dissolved Sb concentration. Interestingly, the Sb isotopic signature at G2 also differed from that measured in the drinking water at the Collet de Deze village (DW, δ^{123}Sb = 0.62‰) which is enriched with Sb (3.9 µg Sb.L^{-1}). This tap water which was pumped in the Dourdon and Gardon Sb-rich alluvial aquifer and delivered without any treatment for Sb removal may reflect the isotopic signature of the natural geogenic Sb source.

Downstream from the station G2, the Sb isotopic composition did not change significantly until station G4, with an average signature of 0.72 ± 0.01‰. Input of tributary T2, that exhibited lower Sb concentration (0.6 µg.L^{-1}) and Sb isotopic signature (δ^{123}Sb = 0.60‰) did not affect this average δ^{123}Sb value. Such a stable isotopic signature along the course of the Gardon of Alès River associated to a three-fold decrease of Sb concentration suggests a simple dilution of Sb along the river flow or a lack of fractionation during adsorption of Sb onto suspended particles and sediments. Further downstream, Sb isotopic composition decreased slightly from 0.72‰ at station G4 to 0.65‰ at station G5, with no change of Sb concentration (2.4 µg Sb.L^{-1}), suggesting a contribution of lower Sb isotopic signature from T3 tributary (1.9 µg Sb.L^{-1}, δ^{123}Sb = 0.33‰), although this result should be treated with caution since variation was within analytical uncertainty. There was no further change of Sb isotopic signature downstream from the junction with the Gardon of Anduze River (δ^{123}Sb = 0.62‰ at G6), despite the lower δ^{123}Sb value of this tributary (δ^{123}Sb = 0.31‰ at T5), in relation with the low Sb concentration of the Gardon of Anduze River (0.4 µg Sb.L^{-1}). It is noteworthy that the Sb isotopic signature of the Gardon of Anduze River at T5 station (δ^{123}Sb = 0.31‰) matched that of the Amous River tributary that drains the Pb/Zn Carnoulès mine (T4, δ^{123}Sb = 0.27‰).

5. Discussion

5.1. Antimony isotopes and mobilization processes in mine-affected streams

A summary of the Sb isotopic composition (δ^{123}Sb in ‰) reported in this study and in the literature is supplied in Figure 3. The range of δ^{123}Sb values observed in this study extended up to ~0.9‰. Extreme δ^{123}Sb values (-0.06‰ and 0.83‰) were recorded for creeks draining former Sb mines (T1, O1) where the main exploited Sb ore was stibnite (Sb_2S_3). This wide range of Sb isotopic composition was comparable to that reported for stibnite from various countries (~1‰) but it was wider than the range reported for different stibnite samples from a single location (i.e. ~ 0.25‰ for Independence Mountains, Nevada, USA), (Figure 3, Lobo et al. 2012). These contrasted signatures of Sb mine-affected creeks (T1 and O1) might then reflect the difference in isotopic composition of local stibnite, although additional Sb-bearing minerals in the ore might also contribute to the Sb isotopic signature of these creeks. In this respect, numerous rare Pb/Sb sulfosalts (e.g. boulangerite $Pb_5Sb_4S_{11}$, plagionite $Pb_5Sb_8S_{17}$) and tetrahedrite ($Cu_{10}(FeZn)_2Sb_4S_{13}$) have been found besides stibnite at the Bournac mine (upstream from the station O1) (Munoz and Shepherd 1987). Smelting of Sb ore documented for Felgerette mine (BRGM, SIG Mines website) may also have generated residual slags of heavier Sb isotopic signature, as seen for Cd (Cloquet et al. 2005), Hg (Stetson et al. 2009; Yin et al. 2013) and Zn isotopes (Sivry et al. 2008; Sonke et al. 2008). These slags may have also contributed to the heavier signature of the Sb mine-impacted creek at station T1 (δ^{123}Sb = 0.83‰). Alternatively, biogeochemical processes involved in Sb mobilization from the ore material to the water may have modified the initial Sb isotopic composition. These processes involve the oxidative dissolution of Sb_2S_3(s) and subsequent release of Sb(III) into water in the form of $Sb(OH)_3$(aq) (Biver and Shotyk, 2012), then Sb(III) may precipitate in the form of Sb(III) oxides and Sb(III)–Fe oxides (Filella et al. 2009), or oxidize into Sb(V), this latter species precipitating possibly in the form of Sb(V)-Fe oxide (Filella et al. 2009; Mitsunobu et al. 2010). Both Sb(III) and Sb(V) species may also sorb onto Fe minerals commonly encountered in mine drainage such as schwertmannite (Manaka et al. 2007), ferrihydrite and goethite (Mitsunobu et al. 2010), or other Fe-, Mn- and Al-hydrous oxides (Thanabalasingam and Pickering 1990). In our study, the predominance of Sb(V) in the creeks impacted by Sb mines suggests that oxidation of Sb(III) into Sb(V) occurred subsequently to stibnite dissolution. Thus, the wide range of Sb isotopic compositions for our Sb mine-impacted creeks are probably not representative of the Sb

signatures in the original stibnite but rather resulted from a combination of processes (dissolution, oxidation, precipitation and adsorption) that may generate fractionation during Sb transport from the ore material into the creek. In this respect, Rouxel et al. (2003) highlighted that the abiotic reduction of Sb(V) into Sb(III) strongly fractionated Sb isotopes with the residual Sb(V) species enriched in the heavier Sb isotope with an instantaneous fractionation factor of 0.9‰, thus redox reactions are expected to fractionate Sb isotopes. In a geochemical context similar to our study (stibnite deposit, near-neutral pH), Tanimizu et al. (2011) showed a difference of 0.30‰ between stibnite from mine dumps of the Ichinokawa mine, Japan, and the corresponding drainage water, the latter being enriched in the heavier ^{123}Sb isotope (Figure 3). This fractionation was attributed to the preferential adsorption of ^{121}Sb isotope onto Fe-hydroxides (Tanimizu et al. 2011). Laboratory experiment of Sb(V) species adsorption onto ferrihydrite also showed a preferential adsorption of ^{121}Sb isotope (Araki et al. 2009). A later study revealed that 16 to 40% of Sb was in the reduced form Sb(III) in sediments of the Ichinokawa River downstream from the Sb mine (Asaoka et al. 2012), therefore, both Sb(III) oxidation and adsorption or precipitation of Sb(III) and Sb(V) species might be involved in Sb isotope fractionation at this site.

The creeks that drained Pb/Zn mines (T2, T3 and T4) also exhibited a wide range of Sb isotopic signatures, from 0.27 to 0.60‰. That may be related to the mineralogy of Sb-bearing phases in the exploited ore. At the Carnoulès mine, which impacts the Amous River (T4), Sb is mainly associated to pyrargyrite (Ag_3SbS_3) and galena (PbS) (Alkaaby 1986). The fate of Sb at the outlet of the tailings impoundment has been investigated at this site (Resongles et al. 2013). Antimony(III) was the predominant species (up to 70%) in the acid mine drainage (AMD) at the outlet of the tailings impoundment. Antimony(III) oxidation occurred along the AMD flow, as well as removal of Sb(III) and Sb(V) species with Fe precipitates and there was no more Sb(III) in the alkaline Amous river that receives the AMD (Resongles et al. 2013). These processes may affect Sb isotopic signature, as seen earlier; therefore, it is unlikely that the δ^{123}Sb value of 0.27‰ measured in the Amous River (T4) reflected the isotopic composition of the initial Sb geological source. Altogether, these results suggest that the creeks that drained Sb- and Pb/Zn mines have probably lost the original Sb isotopic signature of the primary Sb-bearing minerals.

5.2. Antimony isotopes and transport processes in the downstream hydrosystem

Along the Orb River, the variation in Sb isotopic signature, from the Sb mine-affected creek at O1 to the Orb River at O3 (variation of +0.17‰) is difficult to interpret due to the lack of knowledge on possible additional Sb sources and unknown geochemical background value. Nevertheless, a previous study revealed that Sb was affected by mobilization processes in a small pond located in the Bournac Creek downstream from the station O1 (Casiot et al. 2007). The water column of this pond presented oxic conditions and higher dissolved Sb concentration than in the Bournac Creek. Laboratory experiment revealed that Sb can be released from the sediment into the aqueous phase probably due to the oxidation of small pyrite grains in the pond (Casiot et al. 2007). Such processes could explain the change in Sb isotopic composition. In addition, Sb isotope fractionation could occur in the Avene Lake, located in the course of the Orb River, due to the complex biogeochemical processes that take place in such environment. In particular, early diagenesis in lake sediments may affect Sb mobility. Dissolution of Mn- and Fe-oxyhydroxides under anoxic conditions in the sediments can lead to the release of Sb previously sorbed onto these phases; then dissolved Sb concentration is mainly controlled by adsorption onto iron sulfides (Chen et al. 2003). Furthermore, microbiological Sb(V) reduction and subsequent precipitation of Sb(III)-sulfide phases have already been reported in anoxic lake sediments (Kulp et al. 2014).

In the Gardon of Alès River, an important increase of both δ^{123}Sb signature (+0.51‰) and Sb concentration (from 0.4 to 7.7 µg.L^{-1}) occurred on the uppermost course of the river, between station G1 and station G2 (Figure 2b). Such concentration increase has already been observed in stream sediments and surface waters (Resongles et al. 2014, Resongles et al. under review). Besides a possible anthropic origin related to ancient mining activity, Sb was also naturally enriched in groundwater (BRGM, ADES website) and sediments (Resongles et al. 2014) due to the presence of Sb mineralized veins. However, the δ^{123}Sb value at station G2 (δ^{123}Sb = 0.74‰) differed from that of the mine-impacted stream T1 (δ^{123}Sb = 0.83‰) and from the drinking water DW that represented groundwater from the Sb-rich alluvial aquifer (δ^{123}Sb = 0.62‰); both concentrated with Sb (87.4 µg.L^{-1} at T1 and 3.9 µg.L^{-1} at DW). This suggested that Sb in the Gardon of Alès River resulted from a mixing between a natural and a mining source. Alternatively, such difference between surface water (G2) and natural (DW) or mining (T1) sources may suggest fractionation of Sb isotopes during Sb transport.

Further downstream along the Gardon of Alès River, from station G2 to station G6, there was a slight decrease of δ^{123}Sb value (variation of -0.12‰), although it remained stable from G2 to G4 stations (Figure 2b). This pattern was allied to a general decrease of dissolved Sb concentration. Such Sb concentration decrease was also observed previously in stream sediments (Resongles et al. 2014), in water and in suspended particulate matter (Resongles et al. under review). It pointed out the mineralized area on the upper Gardon of Alès River as the main source of Sb in this watershed and the occurrence of dilution and possible natural attenuation at downstream sites along the Gardon of Alès River. However, in natural oxic near-neutral waters, Sb is known to have a fairly weak affinity for suspended particulate matter and is present almost exclusively in the dissolved phase (Filella et al. 2002b, Filella 2011). Such a trend has been observed in the Gardon River where Sb was found mainly associated to the dissolved fraction, even under high flow condition and there was no change in the partitioning between the dissolved and particulate phases along the flow (Resongles et al. under review). Considering the physico-chemical conditions in the main stream of the Gardon River reported in this study (near neutral pH, iron concentration lower than 50 $\mu g.L^{-1}$ (Table 3), organic matter concentration lower than 1 $mg.L^{-1}$ (unpublished data), predominance of Sb(V), suspended particulate matter concentration lower than 5 $mg.L^{-1}$), it is likely that Sb is transported conservatively along the course of the Gardon of Alès River. These results are supported by Sb isotopic composition which was stable from G2 to G4 stations and only slightly decreased at station G5 probably due to the influence of the lower signature of the Avène River (T3). In the same way, in the Gardon of Anduze River (T5) downstream from the Amous River input (T4), Sb isotopic composition was similar to that of the Amous River suggesting conservative Sb transport from T4 to T5, although additional source of similar Sb isotopic signature may have contributed to the Sb load at station T5. Similarly, Asaoka et al. (2011) did not observe any change in Sb isotopic composition between the Ichinokawa River (113 $\mu g\ Sb.L^{-1}$), impacted by one of the highest stibnite output in the world, and the Kamo River (1.5 $\mu g\ Sb.L^{-1}$), which receives the Ichinokawa River. These results suggest that Sb isotopes could help in tracing sources in rivers at distance from mining sites.

Finally, downstream from the confluence between the Gardon of Alès River and the Gardon of Anduze River, at G6 station, Sb isotopic signature (0.62‰) was close to that of the Gardon of Alès River upstream from the confluence at G5 (0.65‰), and significantly different from that of the Gardon of Anduze River at T5 (0.31‰), reflecting the prevailing contribution of the Gardon of Alès River to downstream Sb contamination. Based on the

isotopic signature and considering a simple mixing model between the two rivers, the Gardon of Alès River contribution to the total dissolved Sb load at G6 station was about 90%.

6. Conclusion

In this study, Sb isotopic composition has been determined in water from two mine-affected watersheds: the upper Orb River and the Gardon River in southern France. Prior to isotopic analysis, Sb was preconcentrated and purified from water samples using an original method with thiol-cellulose powder. Antimony isotope ratio was determined using MC-ICP-MS coupled with hydride generation. The instrumental mass bias was corrected using the standard-sample bracketing method and the external reproducibility for $\delta^{123}Sb$ value was 0.06‰ (2σ).

This work demonstrated that significant isotopic variations exist in surface waters both between different hydrosystems and within a single watershed. Isotopic composition ($\delta^{123}Sb$) varied from -0.06‰ to +0.11‰ in the upper Orb River and from +0.23‰ to +0.83‰ in the Gardon River watershed. Various processes are involved in the transfer of Sb from primary minerals to rivers. Therefore, Sb isotopic signature measured in mine-affected streams probably differed from that of the original Sb ore. Nevertheless, Sb isotopic composition appeared to be stable along the Gardon River continuum which is contaminated with Sb. This pattern was attributed to the conservative transport of Sb in this system due to the relative mobile behavior of Sb(V) in natural oxic waters.

Although it is difficult at present time to clarify the causes of isotopic variations observed among the various mining-impacted streams, the magnitude of the range of variation makes Sb isotopic composition a potentially promising tool to study Sb sources and/or biogeochemical processes in hydrosystems. However, further studies are needed to identify and characterize Sb isotope fractionation resulting from the different biogeochemical processes which occur during the release and the transport of Sb in rivers, to ultimately use Sb isotopes for sources or processes tracking.

Acknowledgments

The authors would like to thank Sophie Delpoux for laboratory analysis. This study was supported by the EC2CO-INSU program.

References

Alkaaby, A., 1986. Conglomérats minéralisés (Pb-Ba-Fe) du Trias basal sur la bordure sud-est des Cévennes : exemple du système fluvial en tresse de Carnoulès (Gard). Thesis Université des Sciences et Techniques du Languedoc, p.154.

Araki, Y., Tanimizu, M., Takahashi, Y., 2009. Antimony isotopic fractionation during adsorption on ferrihydrite. Geochimica Cosmochimica Acta 73, A49.

ARS Agence Régionale de Santé du Languedoc-Roussillon. Qualité des Eaux de Boisson. Last accessed on 8/12/2014, http://www.ars.languedocroussillon.sante.fr/.

Asaoka, S., Takahashi, Y., Araki, Y., Tanimizu, M., 2011. Preconcentration method of antimony using modified thiol cotton fiber for isotopic analyses of antimony in natural samples. Analytical Science 27, 25–28.

Asaoka, S., Takahashi, Y., Araki, Y., Tanimizu, M., 2012. Comparison of antimony and arsenic behavior in an Ichinokawa River water–sediment system. Chemical Geology 334, 1–8.

Biver, M., Shotyk, W., 2012. Stibnite (Sb_2S_3) oxidative dissolution kinetics from pH 1 to 11. Geochimica et Cosmochimica Acta 79, 127–139.

Borrok, D.M., Wanty, R.B., Ridley, W.I., Lamothe, P.J., Kimball, B.A., Verplanck, P.L., Runkel, R.L., 2009. Application of iron and zinc isotopes to track the sources and mechanisms of metal loading in a mountain watershed. Applied Geochemistry 24, 1270–1277.

BRGM, SIG Mines. Last accessed on 8/12/2014, http://sigminesfrancebrgmfr/.

BRGM, ADES. Portail National d'Accès aux Données sur les Eaux Souterraines. Last accessed on 8/12/2014, http://www.ades.eaufrance.fr/.

Byrd, J., 1990. Comparative geochemistries of arsenic and antimony in rivers and estuaries. Science of the Total Environment 98, 301–314.

Casiot, C., Ujevic, M., Munoz, M., Seidel, J.L., Elbaz-Poulichet, F., 2007. Antimony and arsenic mobility in a creek draining an antimony mine abandoned 85 years ago (upper Orb basin, France). Applied Geochemistry 22, 788–798.

Casiot, C., Egal, M., Elbaz-Poulichet, F., Bruneel, O., Bancon-Montigny, C., Cordier, M.-A., Gomez, E., Aliaume, C., 2009. Hydrological and geochemical control of metals and arsenic in a Mediterranean river contaminated by acid mine drainage (the Amous River, France); preliminary assessment of impacts on fish (Leuciscus cephalus). Applied Geochemistry 24, 787–799.

CEC (Council of the European Communities), 1976. Council Directive 76/Substances Dicharged into Aquatic Environment of the Community. Official Journal of the European Communities: Legislation 129, 23–29.

Chang, T.-L., Qian, Q.-Y., Zhao, M.-T., Wang, J., 1993. The isotopic abundance of antimony. International Journal of Mass Spectrometry and Ion Processes 123, 77–82.

Chen, Y.W., Deng, T.L., Filella, M., Belzile, N., 2003. Distribution and early diagenesis of antimony species in sediments and porewaters of freshwater lakes. Environmental Science & Technology 37, 1163–1168.

Cloquet, C., Rouxel, O., Carignan, J., Libourel, G., 2005. Natural Cadmium Isotopic Variations in Eight Geological Reference Materials (NIST SRM 2711, BCR 176, GSS-1, GXR-1, GXR-2, GSD-12, Nod-P-1, Nod-A-1) and Anthropogenic Samples, Measured by MC-ICP-MS. Geostandards and Geoanalytical Research 29, 95–106.

Cloy, J.M., Farmer, J.G., Graham, M.C., MacKenzie, A.B., Cook, G.T., 2005. A comparison of antimony and lead profiles over the past 2500 years in Flanders Moss ombrotrophic peat bog, Scotland. Journal of Environmental Monitoring 7, 1137–1147.

Coplen, T.B., 2011. Guidelines and recommended terms for expression of stable-isotope-ratio and gas-ratio measurement results. Rapid Communications in Mass Spectrometry 25, 2538–2560.

606 Elwaer, N., Hintelmann, H., 2008. Selective separation of selenium (IV) by thiol cellulose powder and
607 subsequent selenium isotope ratio determination using multicollector inductively coupled plasma mass
608 spectrometry. Journal of Analytical Atomic Spectrometry 23, 733-743.
609 Filella, M., Belzile, N., Chen, Y., 2002a. Antimony in the environment: a review focused on natural waters: I.
610 Occurrence. Earth-Science Reviews 57, 125–176.
611 Filella, M., Belzile, N., Chen, Y., 2002b. Antimony in the environment: a review focused on natural waters: II.
612 Relevant solution chemistry. Earth-Science Reviews 59, 265–285.
613 Filella, M., Philippo, S., Belzile, N., Chen, Y., Quentel, F., 2009. Natural attenuation processes applying to
614 antimony: a study in the abandoned antimony mine in Goesdorf, Luxembourg. Science of the Total
615 Environment 407, 6205–6216.
616 Filella, M., 2011. Antimony interactions with heterogeneous complexants in waters, sediments and soils: A
617 review of data obtained in bulk samples. Earth-Science Reviews 107, 325–341.
618 Foucher, D., Ogrinc, N., Hintelmann, H., 2009. Tracing mercury contamination from the Idrija mining region
619 (Slovenia) to the Gulf of Trieste using Hg isotope ratio measurements. Environmental Science &
620 Technology 43, 33–39.
621 Gaillardet, J., Viers, J., Dupré, B., 2003. Trace elements in river waters. Treatise on Geochemistry 5, 225–272.
622 He, M., Wang, X., Wu, F., Fu, Z., 2012. Antimony pollution in China. Science of the Total Environment 421-
623 422, 41–50.
624 Henden, E., İşlek, Y., Kavas, M., Aksuner, N., Yayayürük, O., Çiftçi, T.D., İlktaç, R., 2011. A study of
625 mechanism of nickel interferences in hydride generation atomic absorption spectrometric determination of
626 arsenic and antimony. Spectrochimica Acta Part B 66, 793–798.
627 Hong, S., Soyol-Erdene, T.O., Hwang, H.J., Hong, S.B., Hur, S.D., Motoyama, H., 2012. Evidence of global-
628 scale as, Mo, Sb, and Tl atmospheric pollution in the antarctic snow. Environmental Science &
629 Technology 46, 11550–11557.
630 Hiller, E., Lalinská, B., Chovan, M., Jurkovič, L., Klimko, T., Jankulár, M., Hovorič, R., Šottník, P., Flaková, R.,
631 Ženišová, Z., Ondrejková, I., 2012. Arsenic and antimony contamination of waters, stream sediments and
632 soils in the vicinity of abandoned antimony mines in the Western Carpathians, Slovakia. Applied
633 Geochemistry 27, 598–614.
634 Kimball, B.E., Mathur, R., Dohnalkova, A.C., Wall, A.J., Runkel, R.L., Brantley, S.L., 2009. Copper isotope
635 fractionation in acid mine drainage. Geochimica Cosmochimica Acta 73, 1247–1263.
636 Klee, R.J., Graedel, T.E., 2004. Elemental cycles: A Status Report on Human or Natural Dominance. Annual
637 Review of Environment and Resources 29, 69–107.
638 Krachler, M., Zheng, J., Koerner, R., Zdanowicz, C., Fisher, D., Shotyk, W., 2005. Increasing atmospheric
639 antimony contamination in the northern hemisphere: snow and ice evidence from Devon Island, Arctic
640 Canada. Journal of Environmental Monitoring 7, 1169–1176.
641 Kulp, T.R., Miller, L.G., Braiotta, F., Webb, S.M., Kocar, B.D., Blum, J.S., Oremland, R.S., 2014.
642 Microbiological reduction of Sb(V) in anoxic freshwater sediments. Environmental Science & Technology
643 48, 218–26.
644 Kumar, A.R., Riyazuddin, P., 2010. Chemical interferences in hydride-generation atomic spectrometry. Trends
645 in Analytical Chemistry 29, 166–176.
646 Liu, F., Le, X.C., McKnight-Whitford, A., Xia, Y., Wu, F., Elswick, E., Johnson, C.C., Zhu, C., 2010. Antimony
647 speciation and contamination of waters in the Xikuangshan antimony mining and smelting area, China.
648 Environmental Geochemistry and Health 32, 401–413.
649 Lobo, L., Devulder, V., Degryse, P., Vanhaecke, F., 2012. Investigation of natural isotopic variation of Sb in
650 stibnite ores via multi-collector ICP-mass spectrometry – perspectives for Sb isotopic analysis of Roman
651 glass. Journal of Analytical Atomic Spectrometry 27, 1304-1310.
652 Lobo, L., Degryse, P., Shortland, A., Vanhaecke, F., 2013. Isotopic analysis of antimony using multi-collector
653 ICP-mass spectrometry for provenance determination of Roman glass. Journal of Analytical Atomic
654 Spectrometry 28, 1213-1219.
655 Lobo, L., Degryse, P., Shortland, A., Eremin, K., Vanhaecke, F., 2014. Copper and antimony isotopic analysis
656 via multi-collector ICP-mass spectrometry for provenancing ancient glass. Journal of Analytical Atomic
657 Spectrometry 29, 58-64.
658 Manaka, M., Yanase, N., Sato, T., Fukushi, K., 2007. Natural attenuation of antimony in mine drainage water.
659 Geochemical Journal 41, 17–27.

660 Mitsunobu, S., Takahashi, Y., Terada, Y., Sakata, M., 2010. Antimony(V) incorporation into synthetic
661 ferrihydrite, goethite, and natural iron oxyhydroxides. Environmental Science & Technology 44, 3712–
662 3718.
663 Munoz, M., Shepherd, T., 1987. Fluid inclusion study of the Bournac polymetallic (Sb-As-Pb-Zn-Fe-Cu...) vein
664 deposit (Montagne Noire, France). Mineralium Deposita 22, 11–17.
665 Resongles, E., Casiot, C., Elbaz-Poulichet, F., Freydier, R., Bruneel, O., Piot, C., Delpoux, S., Volant, A.,
666 Desoeuvre, A., 2013. Fate of Sb(V) and Sb(III) species along a gradient of pH and oxygen concentration in
667 the Carnoulès mine waters (Southern France). Environmental Science Processes & Impacts 15, 1536–
668 1544.
669 Resongles, E., Casiot, C., Freydier, R., Le Gall, M., Elbaz-Poulichet, F.. Variation of dissolved and particulate
670 metal (Cd, Pb, Tl, Zn) and metalloid (As, Sb) concentrations under varying discharge during a
671 Mediterranean flood in a former mining watershed, the Gardon River (France). Journal of Geochemical
672 Exploration, under review.
673 Resongles, E., Casiot, C., Freydier, R., Dezileau, L., Viers, J., Elbaz-Poulichet, F., 2014. Persisting impact of
674 historical mining activity to metal (Pb, Zn, Cd, Tl, Hg) and metalloid (As, Sb) enrichment in sediments of
675 the Gardon River, Southern France. Science of the Total Environment 481, 509–521.
676 Rouxel, O., Ludden, J., Carignan, J., Marin, L., Fouquet, Y., 2002. Natural variations of Se isotopic composition
677 determined by hydride generation multiple collector inductively coupled plasma mass spectrometry.
678 Geochimica Cosmochimica Acta 66, 3191–3199.
679 Rouxel, O., Ludden, J., Fouquet, Y., 2003. Antimony isotope variations in natural systems and implications for
680 their use as geochemical tracers. Chemical Geology 200, 25–40.
681 Sen, I., Peucker-Ehrenbrink, B., 2012. Anthropogenic Disturbance of Element Cycles at the Earth´s Surface.
682 Environmental Science & Technology 46, 8601–8609.
683 Shotyk, W., Cheburkin, A.K., Appleby, P.G., Fankhauser, A., Kramers, J.D., 1996. Two thousand years of
684 atmospheric arsenic, antimony, and lead deposition recorded in an ombrotrophic peat bog profile, Jura
685 Mountains, Switzerland. Earth and Planetary Science Letters 145, E1–E7.
686 Shotyk, W., Krachler, M., Chen, B., 2004. Antimony in recent, ombrotrophic peat from Switzerland and
687 Scotland: Comparison with natural background values (5,320 to 8,020 14C yr BP) and implications for the
688 global atmospheric Sb cycle. Global Biogeochemical Cycles.
689 Shotyk, W., Krachler, M., Chen, B., 2005. Anthropogenic impacts on the biogeochemistry and cycling of
690 antimony. Metal ions in biological systems 44, 171–203.
691 Sivry, Y., Riotte, J., Sonke, J., Audry, S., Schafer, J., Viers, J., Blanc, G., Freydier, R., Dupre, B., 2008. Zn
692 isotopes as tracers of anthropogenic pollution from Zn-ore smelters The Riou Mort–Lot River system.
693 Chemical Geology 255, 295–304.
694 Sonke, J., Sivry, Y., Viers, J., Freydier, R., Dejonghe, L., Andre, L., Aggarwal, J., Fontan, F., Dupre, B., 2008.
695 Historical variations in the isotopic composition of atmospheric zinc deposition from a zinc smelter.
696 Chemical Geology 252, 145–157.
697 Stetson, S.J., Gray, J.E., Wanty, R.B., Macalady, D.L., 2009. Isotopic Variability of Mercury in Ore, Mine-
698 Waste Calcine, and Leachates of Mine-Waste Calcine from Areas Mined for Mercury. Environmental
699 Science & Technology 43, 7331–7336.
700 Tanimizu, M., Araki, Y., Asaoka, S., Takahashi, Y., 2011. Determination of natural isotopic variation in
701 antimony using inductively coupled plasma mass spectrometry for an uncertainty estimation of the
702 standard atomic. Geochemical Journal 45, 27–32.
703 Thanabalasingam, P., Pickering, W.F., 1990. Specific sorption of antimony (III) by the hydrous oxides of Mn,
704 Fe, and Al. Water, Air, & Soil Pollution 49, 175–185.
705 USEPA, 1984. Antimony, An Environmental and Health Effects Assessment. US Environmental Protection
706 Agency, Office of Drinking Water, Washington, DC.
707 Wang, X., He, M., Xi, J., Lu, X., 2011. Antimony distribution and mobility in rivers around the world's largest
708 antimony mine of Xikuangshan, Hunan Province, China. Microchemical Journal 97, 4–11.
709 Weiss, D., Rehkämper, M., Schoenberg, R., McLaughlin, M., Kirby, J., Campbell, P.G., Arnold, T., Chapman,
710 J., Peel, K., Gioia, S., 2008. Application of nontraditional stable-isotope systems to the study of sources
711 and fate of metals in the environment. Environmental Science & Technology 42, 655–664.
712 Yin, R., Feng, X., Wang, J., Li, P., Liu, J., Zhang, Y., Chen, J., Zheng, L., Hu, T., 2013. Mercury speciation and
713 mercury isotope fractionation during ore roasting process and their implication to source identification of
714 downstream sediment in the Wanshan mercury mining area, SW China. Chemical Geology 336, 72–79.

715 Yu, M.-Q., Liu, G.-Q., Jin, Q., 1983. Determination of trace arsenic, antimony, selenium and tellurium in various
716 oxidation states in water by hydride generation and atomic-absorption spectrophotometry after enrichment
717 and separation with thiol cotton. Talanta 30, 265–270.
718 Yu, M., Tian, W., Sun, D., Shen, W., Wang, G., Xu, N., 2001. Systematic studies on adsorption of 11 trace
719 heavy metals on thiol cotton fiber. Analytica Chimica Acta 428, 209–218.
720 Yu, M., Sun, D., Tian, W., Wang, G., Shen, W., Xu, N., 2002. Systematic studies on adsorption of trace
721 elements Pt, Pd, Au, Se, Te, As, Hg, Sb on thiol cotton fiber. Analytica Chimica Acta 456, 147–155.
722

Figure captions

Figure 1: Sampling locations a) in the upper Orb River and b) in the Gardon River watershed, Tx represents the stations on tributaries and Gx represents stations on the main stream of the Gardon River (note that the Gardon of Anduze River is considered in this study as a tributary of the Gardon of Alès River despite its most important hydrologic contribution).

Figure 2: Antimony isotopic composition (δ^{123}Sb, in ‰) of water samples in a) the upper Orb River watershed and b) the Gardon River watershed.

Figure 3: Antimony isotopic composition of different environmental and geological materials and anthropogenic samples compiled from literature and reported in this study in the upper Orb River watershed (gray triangle) and in the Gardon River watershed (black triangle). Note that the absolute values of δ^{123}Sb cannot be compared across studies separated by a dash line because the Sb isotopic standard used for the δ^{123}Sb calculation is different.

Table captions

Table 1: Preconcentration and purification procedure. Fraction A: sample solution after its loading on the TCP column; fraction B and C: washing solutions; fraction D: final extract.

Table 2: Instrumental settings and data acquisition parameters for the determination of total trace element concentrations by ICP-MS, Sb concentrations by HG-ICP-MS and Sb isotope ratio measurement by HG-MC-ICP-MS.

Table 3: Water samples characterization: physico-chemical parameters, major and trace element concentrations.

Step	Volume (mL)	Medium	Recovered fraction
1. TCP loading on column	0.7	/	/
2. Cleaning	25	Milli-Q water	/
3. Conditioning	25	0.5 M HCl	/
4. Sample loading	10-500	0.5 M HCl, 0.5 % (w/v) KI-ascorbic acid	A
5. Washing	5	0.5 M HCl	B
6. Washing (purge out the remnant liquid from TCP column at the end of this step)	6	2.5 M HCl	C
7. Transfer of the TCP in a centrifuge tube	/	/	/
8. Sb elution (extraction step repeated three times)	3 x 3 mL	6 M HCl	D
		Ultrasonication for 15min, centrifugation at 4000 rpm for 20 min, recovering of supernantant	

Instrument settings	ICP-MS	HG-ICP-MS	HG-MC-ICP-MS
Intrument	XSeries II, Thermo Scientific	XSeries II, Thermo Scientific	Neptune, Thermo Scientific
RF Power (W)	1400	1400	1290
Gas flow rate ($L.min^{-1}$)			
Cooling	13.0	13.0	15.1
Auxiliary	0.7	0.7	0.9
Sample	0.85	/	/
Sample flow rate ($mL.min^{-1}$)	0.4	/	/
Data acquisition parameters			
Wash time (s)	60	60	120
Uptake time (s)	90	90	100
Number of blocks	3	3	3
Number of cycles per block	20	20	10
Dwell time (ms)	20	20	/
Integration time per cycle (s)	/	/	8
Hydride generation parameters			
System	/	HGX-200 system, CETAC Technologies	
Reagent medium			
Reducing agent	/	1% w/v $NaBH_4$ in 0.05% w/v NaOH	
Sample	/	3 M HCl	
Reagent flow rate ($mL.min^{-1}$)			
Reducing agent	/	1.0	1.0
Sample	/	0.25	0.25
Gas flow rate ($L.min^{-1}$)			
Sample gas	/	0.4	0.5
Add gas	/	0.65	0.6
MC-ICP-MS cup configuration			

C	H1	H2	H3	H4
^{120}Sn	^{121}Sb	^{122}Sn	^{123}Sb	^{126}Te

River	Upper Gardon of Ales River	Gardon of Ales River at Ste Cecile	Gardon of Ales River at La Tour	Gardon of Ales River at Les Promelles	Gardon of Ales River at Vezenobres	Gardon River at Ners	Ravin des Bernes Creek	Grabieux River	Avene River	Amous River	Gardon of Anduze River	Drinking water of the Collet de Deze	Bournac Creek	Avene Lake	Orb River
Station	G1	G2	G3	G4	G5	G6	T1	T2	T3	T4	T5	DW	O1	O2	O3
Temperature (°C)	14.8	16.8	18.9	14.5	13.6	15.8	10.6	15.5	14.6	17.1	14.9	19	9.7	13.7	10.30
pH	6.80	7.26	8.76	8.05	7.92	8.08	7.06	8.01	7.98	8.1	7.6	7.01	7.17	8.34	8.42
Conductivity ($\mu S.cm^{-1}$)	81.3	84.3	630	783	802	474	136.5	658	1747	568	303	89	94.9	424	394
O_2 ($mg.L^{-1}$)	8.8	9.2	14.3	10.5	10.0	9.0	8.6	12.9	9.8	10.8	8.3	8.9	10.3	10.1	12.0
CO_3^{2-} ($mg.L^{-1}$)	n.d.	/	21.97	/	/	/	/	/	/	/	/	/	/	0.04	7.32
HCO_3^- ($mg.L^{-1}$)	n.d.	30.1	182.0	194.7	212.1	169.8	69.4	276.1	236.8	291.2	156.8	30.0	23.4	232.7	216.5
Cl^- ($mg.L^{-1}$)	3.4	3.9	10.7	19.5	26.6	14.7	3.5	14.4	194.4	7.0	6.6	3.7	5.8	5.7	6.0
NO_3^- ($mg.L^{-1}$)	1.1	0.4	/	2.6	4.3	2.2	0.6	2.3	8.0	1.2	0.8	0.6	4.4	3.0	3.0
SO_4^{2-} ($mg.L^{-1}$)	12.3	9.9	202.7	210.1	191.5	95.4	15.4	127.8	455.1	101.3	27.9	10.5	13.0	28.4	24.4
Ca^{2+} ($mg.L^{-1}$)	4.5	6.7	73.1	77.4	87.8	58.6	11.3	113.4	207.7	100.1	36.2	5.9	6.0	50.8	47.0
K^+ ($mg.L^{-1}$)	0.9	0.8	3.2	4.0	5.0	2.8	0.7	2.4	25.8	1.3	1.2	0.7	0.9	1.1	1.0
Mg^{2+} ($mg.L^{-1}$)	3.7	3.6	24.4	25.1	22.0	15.1	8.0	16.5	16.8	24.8	10.4	3.7	4.1	22.8	21.4
Na^+($mg.L^{-1}$)	3.6	3.6	42.0	49.7	47.7	22.4	3.2	16.1	159.2	3.9	5.3	3.9	4.3	4.0	4.0
Ag ($\mu g.L^{-1}$)	0.00	<0.01	<0.01	<0.01	<0.01	<0.01	<0.10	0.06	<0.01	<0.01	<0.01	0.21	0.89	0.17	0.04
Al ($\mu g.L^{-1}$)	2.8	1.1	2.7	6.1	1.0	1.9	3.3	2.8	1.6	53.7	1.7	1.1	10.7	5.4	3.3
As ($\mu g.L^{-1}$)	0.6	1.0	1.4	0.8	1.2	4.6	17.0	2.6	9.0	10.0	6.7	0.5	90.4	7.7	7.4
Ba ($\mu g.L^{-1}$)	42.2	49.1	53.2	54.9	61.8	49.4	28.7	62.1	94.6	52.6	39.6	39.6	82.8	33.2	29.3
Cd ($\mu g.L^{-1}$)	0.02	0.01	0.01	0.18	0.05	0.02	<0.002	0.03	0.43	1.01	0.01	0.02	0.98	0.04	0.03
Co ($\mu g.L^{-1}$)	0.02	0.06	0.11	0.71	0.15	0.10	<0.03	0.14	0.55	6.60	0.06	0.01	<0.03	0.03	0.02
Cr ($\mu g.L^{-1}$)	0.01	<0.005	0.05	0.09	0.10	0.06	<0.1	0.01	0.08	0.03	0.04	0.01	<0.1	0.07	0.08
Cu ($\mu g.L^{-1}$)	0.4	0.2	0.4	0.3	0.6	0.6	0.2	0.7	2.6	0.7	0.4	122.2	1.9	0.6	0.4
Fe ($\mu g.L^{-1}$)	6.9	43.6	27.2	10.6	12.7	21.7	<1.0	91.3	37.6	5.6	22.7	41.7	35.8	3.8	2.6
Ge ($\mu g.L^{-1}$)	0.006	<0.003	0.016	0.014	0.012	0.006	<0.03	0.009	0.017	0.004	<0.003	0.004	<0.03	<0.003	<0.003
Mn ($\mu g.L^{-1}$)	0.9	23.0	8.5	59.7	11.1	3.7	<0.08	28.6	46.0	305.5	7.7	0.47	0.56	1.5	1.6
Mo ($\mu g.L^{-1}$)	0.13	0.24	1.02	0.77	11.9	4.6	0.06	6.7	772.9	0.36	0.23	0.07	0.10	0.26	0.23
Ni ($\mu g.L^{-1}$)	0.66	0.32	0.31	1.87	1.03	0.60	<0.2	0.75	8.7	7.7	0.28	0.29	1.19	0.39	0.29
Pb ($\mu g.L^{-1}$)	0.04	0.04	0.05	0.03	0.11	0.25	<0.01	0.11	0.26	0.46	0.26	0.68	1.20	0.05	0.02
Rb ($\mu g.L^{-1}$)	1.18	0.89	3.78	7.13	5.39	3.05	0.75	2.18	13.9	1.89	1.43	0.75	1.27	1.04	0.93
Sb ($\mu g.L^{-1}$)	**0.4**	**7.7**	**4.2**	**2.4**	**2.4**	**1.2**	**87.4**	**0.6**	**1.9**	**0.5**	**0.4**	**3.9**	**53.8**	**1.3**	**1.1**
Se ($\mu g.L^{-1}$)	<0.06	0.03	0.08	0.13	0.21	0.14	<0.1	0.10	0.29	0.15	0.04	0.004	<0.1	0.06	0.06
Sn ($\mu g.L^{-1}$)	0.13	<0.005	<0.005	<0.005	<0.005	<0.005	<0.05	<0.01	<0.01	<0.005	<0.005	0.009	<0.05	<0.005	<0.005
Sr ($\mu g.L^{-1}$)	26	23	383	499	466	276	18	811	630	157	125	22	21	169	143
Te ($\mu g.L^{-1}$)	<0.005	<0.005	<0.005	<0.005	<0.005	<0.005	<0.05	<0.01	<0.01	<0.005	<0.005	<0.005	<0.05	<0.005	<0.005
Ti ($\mu g.L^{-1}$)	<0.06	0.09	1.67	1.72	1.61	0.84	0.22	1.00	4.73	0.95	0.26	0.10	0.13	0.34	0.30
Tl ($\mu g.L^{-1}$)	0.004	0.004	0.014	0.25	0.29	0.15	<0.002	1.20	3.86	1.11	0.05	0.001	0.011	0.013	0.010
V ($\mu g.L^{-1}$)	0.05	0.01	0.08	0.06	0.19	0.18	<0.03	0.12	3.83	0.03	0.14	0.03	<0.03	0.27	0.25
Zn ($\mu g.L^{-1}$)	2.67	0.39	0.50	51.8	12.4	2.53	<0.5	5.0	14.2	153.8	0.99	29.5	92.2	4.8	4.1

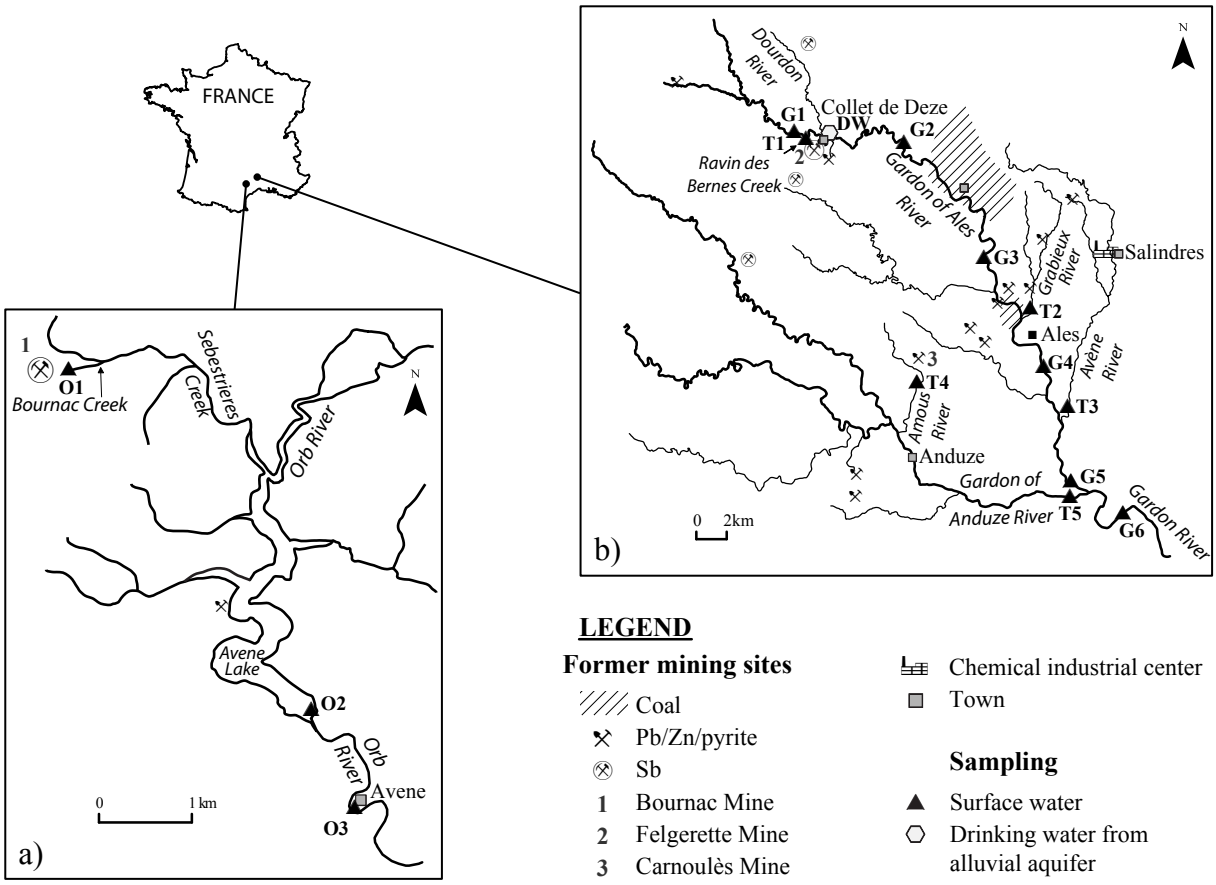
FRANCE
1
O1
Bournac Creek
Sebestrieres Creek
Orb River
N
Avene Lake
O2
Orb River
Avene
O3
0
1 km
a)
Dourdon River
Collet de Deze
G1
DW
G2
T1
2
Ravin des Bernes Creek
Gardon of Ales River
G3
Grabieux River
Salindres
T2
Ales
3
G4
Avène River
T4
T3
Amous River
Anduze
Gardon of Anduze River
G5
T5
G6
Gardon River
0 2km
b)
LEGEND
Former mining sites
Coal
Pb/Zn/pyrite
Sb
1 Bournac Mine
2 Felgerette Mine
3 Carnoulès Mine
Chemical industrial center
Town
Sampling
Surface water
Drinking water from alluvial aquifer

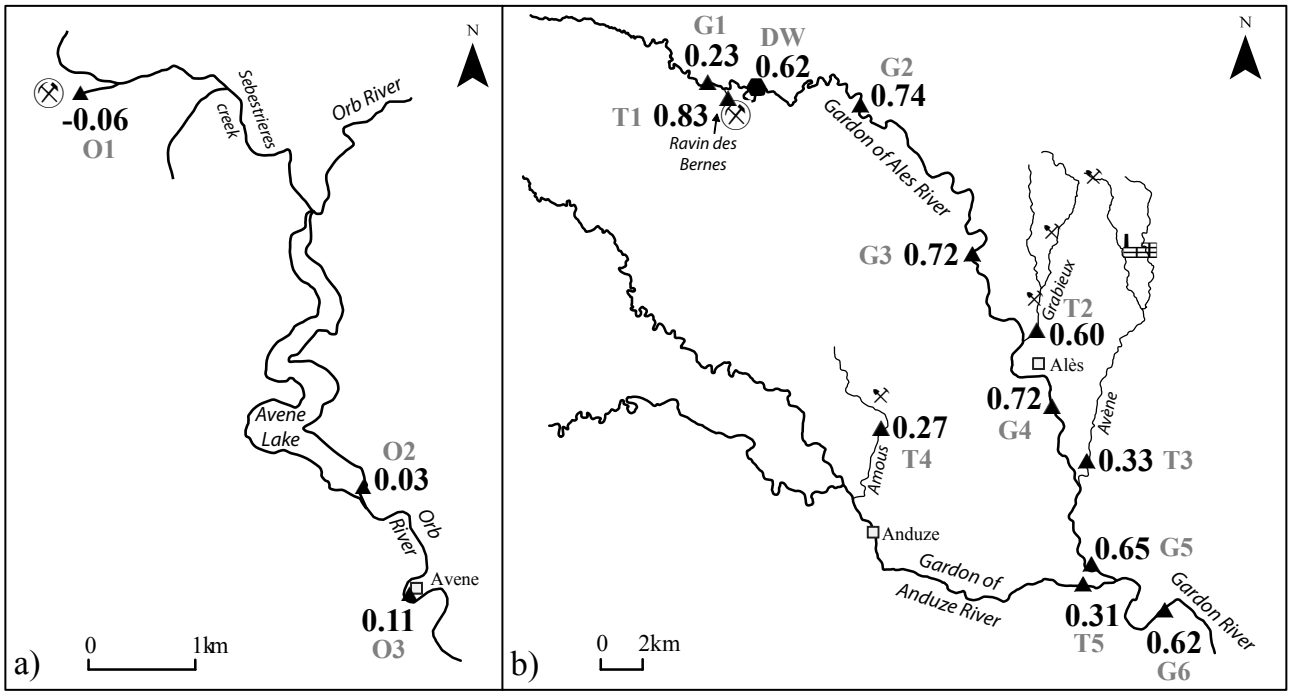

Antimony isotopic signature

0.62 δ^{123}Sb (‰)

▲ River water

⬣ Tap water from the alluvial aquifer

Former mining sites

Pb/Zn

Sb

Chemical industrial center

Town

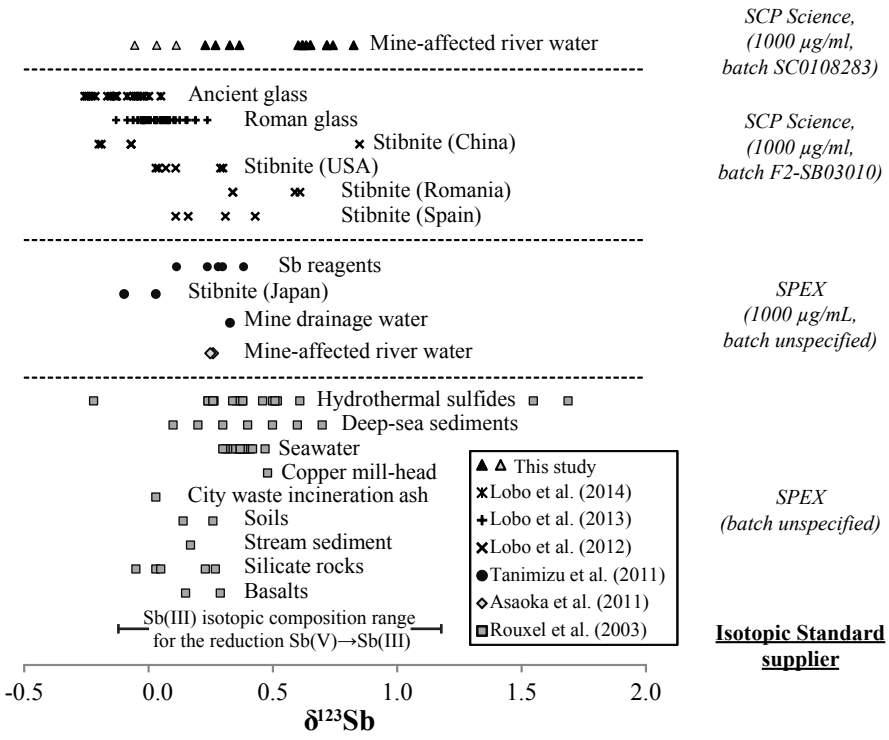
Mine-affected river water
Ancient glass
Roman glass
Stibnite (China)
Stibnite (USA)
Stibnite (Romania)
Stibnite (Spain)
Sb reagents
Stibnite (Japan)
Mine drainage water
Mine-affected river water
Hydrothermal sulfides
Deep-sea sediments
Seawater
Copper mill-head
City waste incineration ash
Soils
Stream sediment
Silicate rocks
Basalts
Sb(III) isotopic composition range for the reduction Sb(V)→Sb(III)
This study
Lobo et al. (2014)
Lobo et al. (2013)
Lobo et al. (2012)
Tanimizu et al. (2011)
Asaoka et al. (2011)
Rouxel et al. (2003)
-0.5
0.0
0.5
1.0
1.5
2.0
δ123Sb
SCP Science, (1000 µg/ml, batch SC0108283)
SCP Science, (1000 µg/ml, batch F2-SB03010)
SPEX (1000 µg/mL, batch unspecified)
SPEX (batch unspecified)
Isotopic Standard supplier

Supporting Information

SI, Figure 1: Effect of the number of Sb extraction step on procedure yield (n=3). Four extractions were successively performed and collected separately. Antimony concentration was determined in each single extract. Antimony recovery was respectively 64 ± 9%, 25 ± 6%, 7 ± 2% and 2 ± 1%. Results showed that three extraction steps were sufficient to achieve a quantitative recovery of Sb (96 ± 2%, n=3), the fourth extraction only slightly improved the procedure yield. Therefore, Sb was recovered by extracting TCP three times using 3 mL of 6N HCl followed by ultrasound treatment.

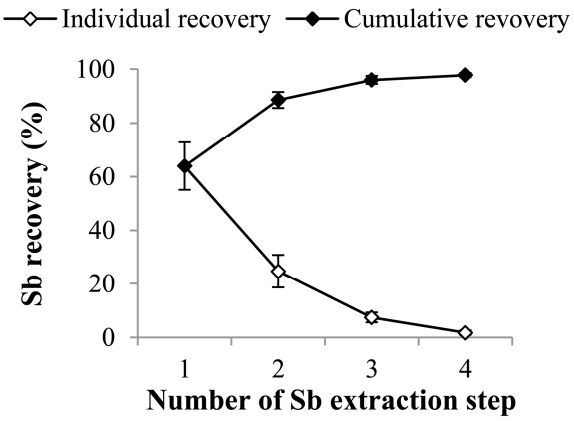

SI, Table 1: Procedure yield of the TCP procedure according to the water volume loaded on TCP column; each sample volume tested was processed in triplicate following the procedure described in section 3.3.b. A sample of river water representative of the average composition of our samples (water sampled at the G5 station, Figure 1, Table 3) was used for this test. Results showed that TCP procedure was reliable and efficient for a large range of river water volumes. This test also demonstrated that small amount of Sb (~20 ng) can be quantitatively recovered from TCP and that at least up to 1200 ng of Sb can be treated with this method.

Processed water volume (mL)	Amount of Sb loaded on TCP (ng)	TCP procedure yield (%) (n=3)
10	24	97 ± 1
50	120	97 ± 3
100	240	98 ± 4
200	480	101 ± 6
500	1200	100 ± 4

SI, Table 2: Recovery of Sb and interfering elements in fractions A, B, C and D collected at each step of the TCP procedure. Ten mL of the certified water NIST SRM 1643e and 10 mL of an experimental solution spiked with As, Ge, Sb, Se, Sn and Te at 50 $\mu g.L^{-1}$ each were used. Each sample was processed in triplicate following the TCP procedure described in section 3.3.b. During this experiment, all fractions (A, B, C and D) were collected and analyzed for Sb and interfering element concentrations. Results showed that metals (Co, Cr, Fe, Ni, Pb and Zn) passed through the TCP column (fraction A), as expected (Yu et al. 2001; Elwaer and Hintelmann 2008) while As, Sb, Se, Sn and Te were quantitatively retained on TCP (> 98%, Table 4). Cd, Cu and Ge were partially retained on TCP (respectively 19%, 46% and 21%). The two successive washes (Fraction B and C) allowed to remove these elements from TCP. Sn was almost completely retrieved in the fraction C (94 ± 1%) as observed by Asaoka et al. (2011). Finally, Sb was quantitatively recovered in the final extract (fraction D) while other elements were not detectable (As, Cd, Co, Fe, Pb, Zn) or quantitatively separated (≤2% of initial Cr, Cu, Ge, Ni, Sn, Te and 4% of Se).

Element	Initial concentration of sample ($\mu g.L^{-1}$)	Recovered in the solution after loading Fraction A (%)	Recovered in the first washing Fraction B (%)	Recovered in the second washing Fraction C (%)	Recovered in the final extract Fraction D (%)
Certified water SRM 1643e					
Cd	6.6	81 ± 5	7 ± 3	0.5 ± 0.5	<0.02[a]
Co	27	93 ± 0.3	3 ± 0.5	<0.01[a]	<0.01[a]
Cr	20	98 ± 3	3 ± 0.5	1 ± 0.5	2 ± 0.1
Cu	23	54 ± 1	32 ± 1	6 ± 2	1 ± 0.8
Fe	98	103 ± 3	<0.9[a]	<0.2[a]	<0.3[a]
Ni	62	91 ± 1	3 ± 0.2	0.3 ± 0.1	0.5 ± 0.1
Pb	20	101 ± 1	4 ± 0.4	<0.05[a]	<0.2[a]
Sb	58	0.9 ± 0.4	<0.1[a]	<0.01[a]	97 ± 1
Zn	79	89 ± 7	<0.4[a]	<0.1[a]	<5[a]
Experimental solution					
As	50	<2[a]	<1[a]	<1[a]	<2[a]
Ge	48	79 ± 1	7 ± 0.6	0.6 ± 0.01	2 ± 0.1
Sb	50	<2[a]	<2[a]	<1[a]	95 ± 1
Se	50	<1[a]	<0.6[a]	<0.5[a]	4 ± 0.3
Sn	53	<2[a]	<0.3[a]	94 ± 1	2 ± 0.5
Te	49	2 ± 0.4	0.8 ± 0.3	0.2 ± 0.01	2 ± 0.1

[a]Measured concentration below the detection limit value

SI, Table 3: Sb isotope composition of the certified refence water NIST 1643e with duplicated analysis of all procedural replicates

Procedural replicates	**δ^{123}Sb in ‰ (duplicate analysis)**					**Average**	**Standard deviation**	**TCP procedure recovery (%)**
	1	2	3	4	5			
NIST 1643e-1	0.12	0.14	0.11			0.12	0.01	97
NIST 1643e-2	0.18	0.17	0.18	0.15	0.09	0.15	0.04	96
NIST 1643e-3	0.17	0.17	0.07			0.14	0.05	96
NIST 1643e-4	0.21	0.26	0.14	0.14		0.19	0.06	103
NIST 1643e-5	0.20	0.14	0.14			0.16	0.04	101
						0.16	**0.03**	